Synsint Research Group

Research article

Role of Si_3N_4 on microstructure and hardness of hot-pressed ZrB_2−SiC composites

Zahra Bahararjmand [a,*], Mohammad A. Khalilzadeh [b], Farshad Saberi-Movahed [c],
Tae Hyung Lee [d], Jinghan Wang [d], Sea-hoon Lee [e], Ho Won Jang [d]

[a] *Department of Biophysics, Istanbul University-Cerrahpasa, Istanbul, Turkey*

[b] *Department of Forest Biomaterials, College of Natural Resources, North Carolina State University, Raleigh, North Carolina, 27695-8005, United States*

[c] *Department of Materials Science and Engineering, North Carolina State University, Raleigh, North Carolina, 27695-8005, United States*

[d] *Department of Materials Science and Engineering, Research Institute of Advanced Materials, Seoul National University, Seoul 08826, Republic of Korea*

[e] *Division of Powder/Ceramics Research, Korea Institute of Materials Science, Changwon, 51508, Republic of Korea*

ABSTRACT

The impact of Si_3N_4 content on the hardness and microstructural developments of ZrB_2-SiC material has been investigated thoroughly in the present investigation. Having prepared the raw materials in a jar mill, the ZrB_2-SiC samples containing various amounts of Si_3N_4 were hot-pressed at 1850 °C. Furthermore, XRD, FESEM, and HRTEM were utilized to evaluate the microstructure of samples. The formation of in-situ h-BN was proved by the mentioned methods. Also, it was shown that the Vickers hardness of ZrB_2-SiC increases up to 20 GPa in presence of 4.5 wt% Si_3N_4 which is 3 GPa more than the sample without Si_3N_4. Results show that the positive effect of increased relative density on hardness is more than the negative effect of h-BN soft phase formation.

© 2021 The Authors. Published by Synsint Research Group.

1. Introduction

Nowadays, ultra-high temperature ceramics (UHTCs) are used in the cutting-edge technological progresses. ZrB_2 with the hexagonal structure is one of the most applicable UHTCs. ZrB_2 has suitable thermal and mechanical properties, high temperature resistance, high corrosion resistance, and high melting point, which make it a suitable material to be used in high temperature structural applications, e.g., space crafts. Despite all these marvelous properties, ZrB_2 cannot be easily sintered. Furthermore, it is fragile and does not have a good anti-oxidation property. A practical method for solving these problems, which limit the application of ZrB_2, is composing it with other ceramics or metals [1–5].

The most important ZrB_2-based composite is ZrB_2-SiC, which is usually produced by various sintering procedures, i.e., pressure-less sintering, hot-pressing, microwave sintering and so on. SiC improves the sinterability of composite by reducing the surface oxides of ZrB_2. SiC also inhibits the grain growth. Nano-SiC particles not only give the composite more anti-oxidation resistance, but they also create a composite with high bending strength. Although making composite with SiC reduces the limitations of ZrB_2, using dopants in the composite may enhance the mechanical properties in a way that the final product will be even much more applicable [6–9].

There is a huge body of literature studied the microstructure and mechanical features of ZrB_2-SiC in presence of various additives. Si_3N_4 is one of the additives which has the most impact on the structural properties of ZrB_2-SiC composite. By the way, the exact impacts of Si_3N_4 on various characteristics of hot-pressed ZrB_2-SiC materials have not been investigated thoroughly [10, 11].

Liu et al. [12] investigated the improved mechanical properties of laminated ZrB_2–SiC composites with interfacial porous Si_3N_4. They proposed that the notable high-temperature strength of final product may be attributed to the porous Si_3N_4 whisker which absorbs the glassy phase gathered at the crack tip, avoiding grain boundary sliding. Golla et al. [13] studied the oxidation and microstructure behavior of ZrB_2-20 vol% SiC composites introduced by Si_3N_4 and Ta additives using spark plasma sintering at 1900 °C. They concluded that the microstructure of composite is comprised of new secondary phases (BN, ZrN, ZrO_2), together with ZrB_2 and SiC. They also showed that Ta improves the oxidation properties more than Si_3N_4. In another investigation accomplished by Thimmappa et al. [14], oxidation behavior, hardness, and phase stability of SPSed ZrB_2-SiC-Si_3N_4 materials were studied. ZrB_2-20 vol%-SiC-5 vol% Si_3N_4 hardness was determined to be 30.56 GPa. Ahmadi et al. [15] examined the Sintering behavior of ZrB_2–SiC composites doped with Si_3N_4. They showed that relative density increases by the incorporation of Si_3N_4 in hot-pressed specimens. A reverse trend was observed in pressureless sintered composites, owing to the generation of gaseous byproducts, resulting in the entrapment of more pores in the ultimate structure. Zou et al. [16] studied mechanical properties of ZrB_2–20 vol% SiC materials. They evaluated strength on the basis of temperature in terms of the grain sizes, microstructural defects, differences in oxygen content, grain boundary phases, and nature of fracture. Pourmohammadie Vafa et al. [17] investigated graphite introduction on the properties of as-sintered ZrB_2–SiC ceramics. Phase analysis of hot-pressed specimens showed the generation of the in-situ B_4C and Zr_3C_2 phases, along with the original compounds. Shahedi Asl et al. [18] investigated the microstructure of SPSed ZrB_2-based composites introduced by nano-sized SiC dopants using TEM technique. TEM studies confirmed the generation of such phases, which were comprised of a Si–B–O glassy bed with C and ZrC islands distributed therein.

Although some brilliant researches have been carried out on the characteristics of ZrB_2-SiC-Si_3N_4 composites, in this work we have tried to study the microstructure of such composites using polished and fractured surfaces, as well as prepared FIB samples. Moreover, the impact of various Si_3N_4 content on the hardness and sinterability of ZrB_2-SiC has been investigated, too. For this objective, after the preparation of raw materials and hot-pressing process, density and hardness of samples were calculated. Furthermore, XRD, FESEM, and HRTEM were utilized for evaluating the microstructures. The aim of this investigation is to study the structural changes caused by Si_3N_4 in the ZrB_2-SiC composite, which lead to higher hardness values.

2. Experimental procedure

2.1. Starting materials and fabrication method

The raw powders of Si_3N_4, SiC, ZrB_2, and phenolic resin (5 wt%) were employed in this examination as the raw materials. Table 1 provides some useful information associated with these materials. To assess the impact of Si_3N_4 content on the microstructure, sintering behavior, and mechanical characteristics of ZrB_2-SiC substances, four different samples were designed to be fabricated (Table 2). For doing so, at first, the required ingredients for each designed specimen were weighed precisely, and then, were dispersed using a jar-mill facility (ZrO_2 balls and Teflon cup) in the ethanol medium. Subsequently, a rotary evaporation device was used to remove the ethanol medium at 100 °C.

Table 1. The initial powders' data.

Starting powders	Particle size	Purity (%)
ZrB_2	< 3 μm	98.0
SiC	< 6 μm	98.5
Si_3N_4	< 2 μm	99.0

Uniform admixtures were secured by grinding the dried slurries and passing them through a 100-mesh screen. Finally, the prepared mixtures were hot-pressed under 20 MPa at 1850 °C for 90 min.

2.2. Characterization

The relative density values of samples were reported as the proportions of bulk and theoretical densities. The crystalline phases of each composite were examined using an XRD device (PW1800, Philips). Moreover, both fracture and polished surfaces of samples were studied in terms of microstructures, by a FESEM (Mira3, Tescan), coupled with an EDS analyzer. Moreover, a complementary microstructural examination was accomplished by an HRTEM (F20 S-TWIN, Philips). The HSC chemical package was utilized to check the feasibility of the probable chemical reactions over the hot-pressing process. Vickers technique was employed to determine the hardness of hot-pressed samples by exerting 49 N load on the polished surfaces for 14 s. For each specimen, at least six indentations were carried out.

3. Results and discussion

Based on the XRD spectra and FESEM images of as-received ZrB_2, SiC, and Si_3N_4 powders (not shown here), the shape of SiC particles is polyhedral. SiC particles are not agglomerated and they are in the range of 3–10 μm. The size of agglomerated Si_3N_4 is about 1–3 μm. Finally, the size of ZrB_2 is smaller than 5 μm. Powders with different sizes could break down and be put together in a pack during the pressing. In this case, the final product could be close pack and the density of composites will be enhanced. ZrB_2, SiC and Si_3N_4 have hexagonal structures. Furthermore, the XRD patterns of powders roughly show the single-phase high- purity products. Only a single peak for SiO_2 could be detected in the SiC pattern, which could be attributed to the surface oxidation. According to references, there have to be other oxides like B_2O_3, and ZrO_2 on the surface of ZrB_2 [19–25]. The reason for existence of these oxides is due to high oxidation tendency of carbides, borides and nitrides on the surface to be thermodynamically stable [26, 27]. Since the amounts of such oxides are less than other phases (usually under 2.5%), they usually cannot be identified by XRD. Fig. 1 illustrates the relative density of ZrB_2-SiC composites containing various amounts of Si_3N_4. As it is illustrated, the relative density of HPed composites is enhanced by increasing the amount of Si_3N_4. The

Table 2. Coding system and samples' compositions.

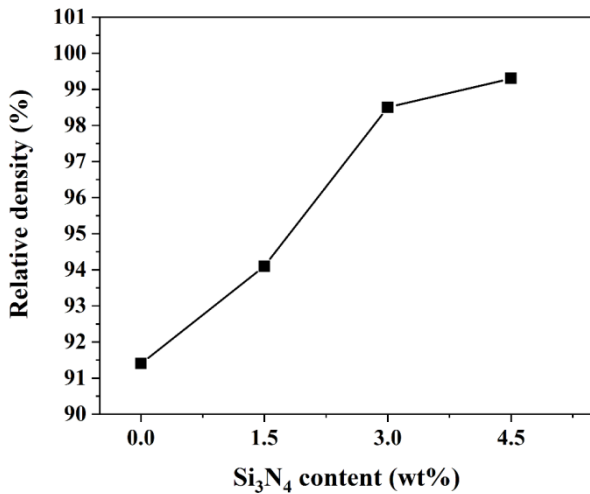| Sample	SiC (vol%)	Si_3N_4 (wt%)
S0	25	0.0
S1.5	25	1.5
S3	25	3.0
S4.5	25	4.5

Fig. 1. The calculated relative density values of samples.

relative density of ZrB_2-SiC composite is about 91.4% after sintering, which reaches 99.3% for the sample containing 4.5 wt% Si_3N_4. The enhanced relative density may enhance the mechanical properties of the final sample. Porosities are the preferred locations for crack propagations, which could reduce the strength and hardness of ceramics. A probable reason for increasing the relative density of ZrB_2-SiC system in the presence of Si_3N_4 additive could be the in-situ generation of some phases that could help the sintering process. A thermodynamic investigation of probable chemical reactions is needed for a better understanding of this phenomenon.

Fig. 2 indicates the XRD patterns of the hot-pressed ceramics containing 3 and 4.5 wt% Si_3N_4. As is indicated, hexagonal ZrB_2 (Reference code: 00-034-0423), SiC (Reference code: 00-031-1232) and BN (Reference code: 01-085-1068) are detected in these patterns. The amount of BN phase is increased by enhancement of the Si_3N_4 content in the sample, which is recognized by the relative intensity of XRD peaks. The only variable among samples is the addition of
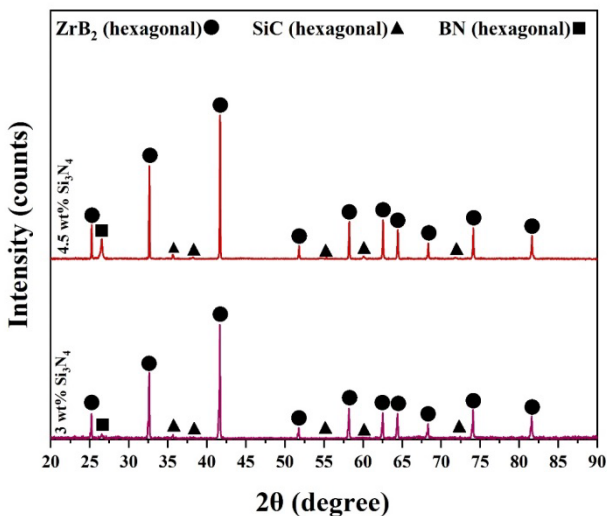
various amounts of Si_3N_4. Therefore, there have to be some chemical reactions between Si_3N_4 and other starting materials for the formation of BN phase.

According to the previously published papers, surfaces of as-received powders, i.e., ZrB_2 and SiC, contain surface oxides, such as SiO_2, B_2O_3 and ZrO_2. In fact, the initial admixture is comprised of ZrB_2, SiC, and Si_3N_4 original phases and the surface oxides of SiO_2, B_2O_3 and ZrO_2. Several chemical interactions may be related to these existing materials which are introduced in Fig. 3.

Fig. 3 shows the Gibbs free energy vs. temperature for the possible chemical reactions in this system. These reactions can take place in the standard pressure of 1 atm; so, in hot-pressing process these reactions may happen in lower temperatures, due to higher applied pressure. The most negative value of Gibbs free energy is for the reaction between Si_3N_4 and B_2O_3 as it is illustrated in Eq. 1.

$$Si_3N_4 + 2B_2O_3 = 4BN + 3SiO_2 \qquad (1)$$

According to Eq. 1, BN can be generated in the interface of ZrB_2/Si_3N_4, because B_2O_3 oxide is available on the surface of ZrB_2 [19–25]. As is illustrated in Fig. 3, within the whole temperature range, the Gibbs free energy of Eq. 1 is the lowest amongst all possible reactions; accordingly, the mentioned reaction occurs while the reactants exist. There is also another reaction between Si_3N_4 and B_2O_3 (Eq. 2), which could progress above 1600 °C by turning the Gibbs free energy towards negative values.

$$Si_3N_4 + B_2O_3 = 2BN + 3SiO(g) + N_2(g) \qquad (2)$$
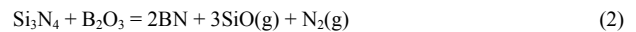
If there is an adequate amount of reactants, Eq. 2 is the second possible equation in this system. Si_3N_4 reacts with SiO_2 to form gaseous SiO and N_2 as well as liquid Si as shown in Eq. 3.

$$Si_3N_4 + SiO_2 = 2SiO(g) + 2Si(l) + 2N_2(g) \qquad (3)$$
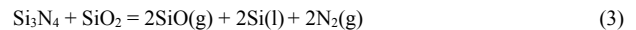
Eq. 3 has a negative Gibbs free energy value above 1700 °C. Therefore, this equation could be the third possible reaction happening in this system. Liquid Si could be helpful in sintering process and a scientific reason for higher relative densities of samples containing Si_3N_4 [28–

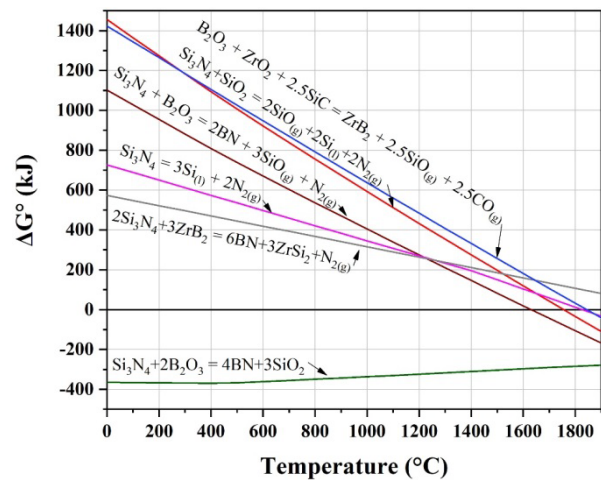**Fig. 2.** The XRD spectra of the hot-pressed samples containing 3 and 4.5 wt% Si_3N_4.

Fig. 3. The temperature dependency of standard Gibbs free energy for some of the noted reactions.

30]. There are also two other reactions which have negative values of Gibbs free energy above 1800 °C. Eq. 4 which forms ZrB_2 and gaseous SiO and CO by reaction amongst B_2O_3, ZrO_2 and SiC.

$$B_2O_3 + ZrO_2 + 2.5SiC = ZrB_2 + 2.5CO(g) + 2.5SiO(g) \qquad (4)$$

Furthermore, Eq. 5 is also feasible at temperatures above 1800 °C. This reaction is the decomposition reaction of Si_3N_4. Liquid Si and N_2 gas would be the products of this equation. As it was mentioned previously, the liquid Si phase derived from Eq. 3 and Eq. 5 is an aid to promote the densification behavior of the final product as exhibited in Fig. 1.

$$Si_3N_4 = 3Si(l) + 2N_2(g) \qquad (5)$$

According to Fig. 2, BN is one of the detected phases formed over hot-pressing process. In the first sight of view, it comes to mind that BN is formed by the direct reaction between Si_3N_4 and ZrB_2 based on Eq. 6. Incidentally, the value of Gibbs free energy for the direct reaction between Si_3N_4 and ZrB_2 is positive even at 1850 °C.

$$2Si_3N_4 + 3ZrB_2 = 6BN + 3ZrSi_2 + N_2(g) \qquad (6)$$
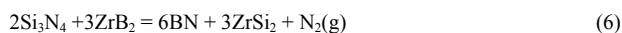
The results show that the final BN detected in XRD patterns of hot-pressed samples is due to a reaction between B_2O_3 oxide on the surface of ZrB_2 and Si_3N_4 additive. Based on Fig. 2, the amount of BN phase will increase by introducing more Si_3N_4 in the composite. This can be concluded from the intensity of BN main peaks of the XRD patterns. As it was noted previously, the only limit for formation of BN is the existence of reactants; therefore, the amount of in-situ formed BN will be increased by incorporating more Si_3N_4.

There should also be some amount of carbon extracted from pyrolyzed resin among reactants. Carbon could react with some ingredients and form other in-situ phases.
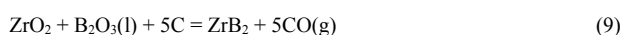
There are two possible reactions between Si_3N_4 and carbon. Eq. 7 shows the reaction amongst Si_3N_4, carbon and ZrB_2, producing two carbides, a nitride and gaseous nitrogen.

$$4C + Si_3N_4 + ZrB_2 = ZrC + 2BN + 3SiC + N_2(g) \qquad (7)$$
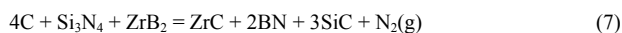
According to [19], Eq. 7 could be feasible above 975 °C. Accordingly, Eq. 7 would be the second chief reaction in this system if enough content of carbon were present. Eq. 7 also relies upon the amount of Si_3N_4 and it would be more favorable with higher Si_3N_4 content. Si_3N_4 additive can also interact with carbon and form N_2 and SiC via Eq. 8:

$$Si_3N_4 + 3C = 3SiC + 2N_2(g) \qquad (8)$$

Eq. 8 is possible at temperatures over 1450 °C, based on the Gibbs free energy values. The remaining carbon could remove oxides from the surface of particles. The existence of oxide phases on the surface of initial particles could be a detrimental factor on grain coarsening over sintering process. Residual carbon can individually reduce oxide impurities, based on the following reactions.

$$ZrO_2 + B_2O_3(l) + 5C = ZrB_2 + 5CO(g) \qquad (9)$$

$$SiO_2 + 3C = SiC + 2CO(g) \qquad (10)$$

$$ZrO_2 + 3C = ZrC + 2CO(g) \qquad (11)$$

These reactions are possible at temperatures higher than 1500 °C. The products of Eq. 9 to Eq. 11 may improve the sinterability of ZrB_2–SiC ceramics. These reactions were also reported in some other researches [19, 31, 32], but it should be considered that the amount of remaining carbon may be diminished, thanks to the progression of several abovementioned reactions. Hence, the advancement of such reactions may be limited by lack of carbon. It was reported that the generation of interfacial fine ZrC ingredient may enhance the sinterability of ZrB_2-based materials [28–30], though it sounds that the resulted CO can impair the densification stage.

According to the above discussion it could be concluded that Eq. 1 can be the main reaction in this system, leading to the in-situ formation of BN. Other reactions may be limited due to the shortage of Si_3N_4 and carbon content. However, small amounts of other in-situ products could be formed during hot-pressing, too. Based on our sight of view, and upon the results of XRD (Fig. 2), the main available phases in the final composites are ZrB_2 and SiC, as well as the in-situ produced BN, which should be studied more by FESEM and HRTEM techniques.

Fig. 4 shows the backscattered FESEM images of the polished ZrB_2-SiC composites containing various amounts of Si_3N_4. As is shown, the remaining pores are detectable in S0, S1.5 and even S3 samples. As was mentioned previously, during sintering process and by increasing the amount of Si_3N_4, liquid Si will form according to Eq. 3 and 5. This liquid phase could remove the porosities and help the composites to be more compact. Furthermore, the existence of Si_3N_4 can trigger some chemical reactions, improving densification.

Fig. 5 shows the backscattered FESEM image of the polished surface of ZrB_2-SiC ceramic containing 4.5 wt% Si_3N_4 additive. A smooth surface without any apparent porosity can be seen in this image. EDS maps show that C, N, O and B are uniformly distributed on the polished surface. As it was mentioned earlier, BN phase is formed in the interfacial area of ZrB_2 and Si_3N_4 particles. Therefore, for the evaluation and illustration of BN, higher magnification is needed.
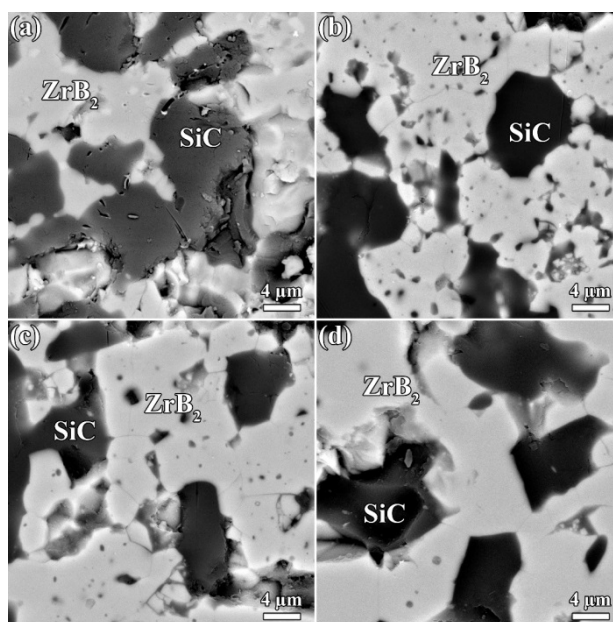

Fig. 4. The backscattered FESEM images from the polished surfaces of the a) S0 b) S1.5, c) S3, and d) S4.5 samples.
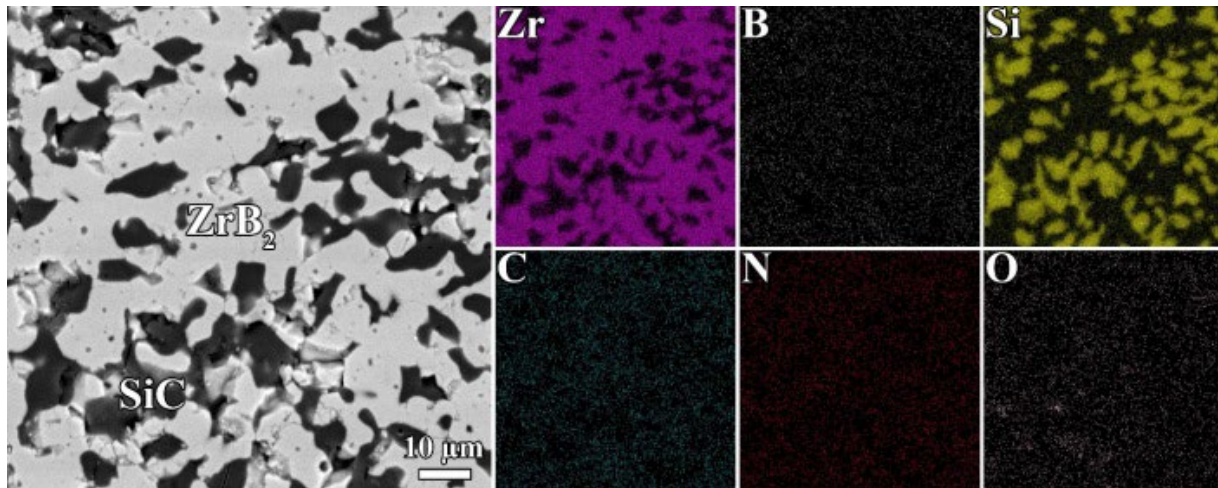
Fig. 5. The backscattered FESEM micrograph from the polished surfaces of the S4.5 sample, together with the corresponding EDS map images.

Fig. 6 shows the backscattered fractograph of S3 sample. As is indicated, the S3 sample is mainly comprised of ZrB_2, and SiC phases, in which some in-situ h-BN compound is formed. In other words, by introducing Si_3N_4 to the composite samples, the BN phase initiates to nucleate on the surface of ZrB_2 where Si_3N_4 particles exist.

Fig. 7 illustrates the HRTEM images of the S4.5 sample. Two different interfaces of SiC and ZrB_2 have been shown in these images. Fig. 7a shows an interface between ZrB_2 and SiC phases. As is shown, there is not any BN or other synthesized phases formed in this interface. This interface has been marked as clean interface. Fig. 7b shows an interface between SiC and ZrB_2 with BN phase between them. It seems that, Si_3N_4 particles convert into BN phase. According to thermodynamic investigations, it seems that the nucleation of BN phase initiates between Si_3N_4 and B_2O_3 on the surface of ZrB_2.

One of the problems associated with composite materials is the weak mechanical junctions in the interfacial areas. Although sintering process helps the diffusion bonding and also promotes chemical reactions at interfaces, these areas mostly have a detrimental impact on mechanical properties. The mentioned h-BN phase synthesized in-situ between SiC and ZrB_2 particles, could even increase this detrimental impact due to its soft nature.

Fig. 8 plots the Vickers hardness values of S0, S1.5, S3 and S4.5 samples. The curve illustrates hardness as a function of Si_3N_4 content. As is clear, the Si_3N_4 incorporation has generally a positive impact on the hardness of specimens. The hardness value for S0 sample is about 17 GPa; however, the S1.5 sample experiences a slight reduction by the addition of 1.5 wt% Si_3N_4. By contrast, the samples get harder by adding more Si_3N_4 content. The most significant Vickers hardness is related to S4.5 sample, standing at 20 GPa.

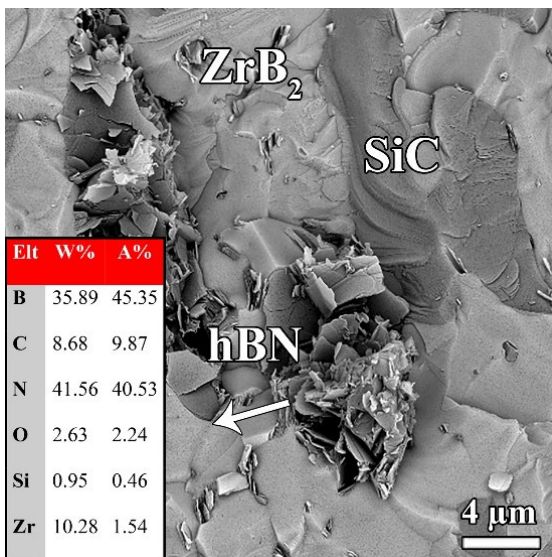As was mentioned earlier, there are two main factors affecting hardness

Elt	W%	A%
B	35.89	45.35
C	8.68	9.87
N	41.56	40.53
O	2.63	2.24
Si	0.95	0.46
Zr	10.28	1.54

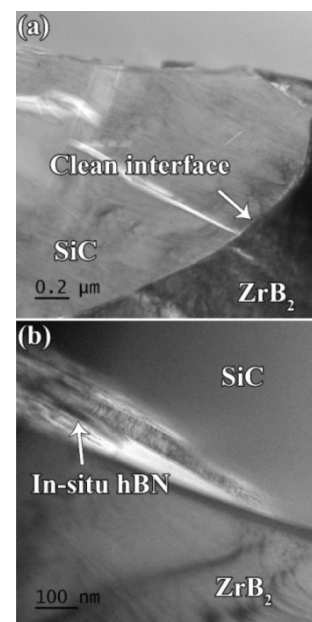**Fig. 6.** The backscattered FESEM fractograph of the S3 sample.

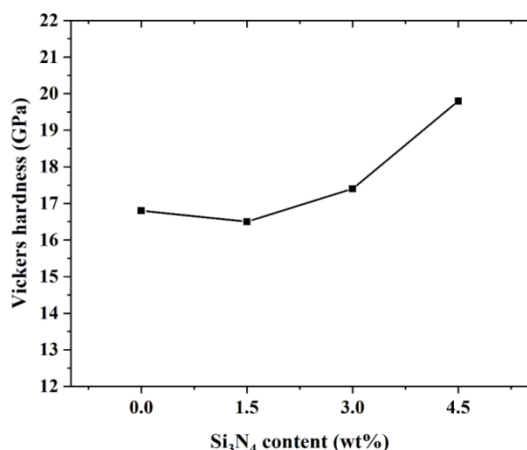**Fig. 7.** The TEM micrographs of the S4.5 samples.

Fig. 8. The Vickers hardness of the hot-pressed samples.

of this composite system, i.e., the improvement of relative density, which has a positive effect and the formation of h-BN, which has a negative effect. It seems that for the S1.5 sample, the effect of h-BN formation is dominant over the enhancement of relative density. However, for the S3 and S4.5 samples, increasing relative density is dominant over the formation of h-BN phase, leading to higher values of Vickers hardness.

4. Conclusions

The impact of Si_3N_4 content on the hardness and microstructural development of ZrB_2-SiC material has been investigated thoroughly in the present investigation. The following results are the main conclusions of this investigation;

- BN phase forms in the interface between SiC and ZrB_2 phases by a reaction between B_2O_3 and Si_3N_4 ingredients.
- The amount of in-situ formed BN will increase by introducing more Si_3N_4.
- Although h-BN is a soft phase, the formation of it in the interface of ZrB_2-SiC composite not only did not decrease the hardness, but also improved this property thanks to the increased relative density.
- The Vickers hardness of ZrB_2-SiC ceramic is about 17 GPa, which increases up to 20 GPa by the addition of 4.5 wt% Si_3N_4.

CRediT authorship contribution statement

Zahra Bahararjmand: Writing – original draft, Conceptualization, Investigation.
Mohammad A. Khalilzadeh: Data curation, Visualization.
Farshad Saberi-Movahed: Methodology, Software.
Tae Hyung Lee: Investigation, Validation.
Jinghan Wang: Methodology, Resources.
Sea-hoon Lee: Project administration.
Ho Won Jang: Supervision, Writing – review & editing.

Data availability

The data underlying this article will be shared on reasonable request to the corresponding author.

Declaration of competing interest

The authors declare no competing interests.

Funding and acknowledgment

References

[1] K. Shugart, Oxidation Behavior of Zirconium Diboride Silicone Carbide Based Materials at Ultra-High Temperatures, PhD Thesis, University of Virginia, Charlottesville, Virginia. (2014). https://doi.org/10.18130/V3K51P.

[2] R.V. Krishnarao, G. Madhusudhan Reddy, Gas tungsten arc welding of ZrB2–SiC based ultra high temperature ceramic composites, Def. Technol. 11 (2015) 188–196. https://doi.org/10.1016/j.dt.2015.03.002.

[3] M. Jaberi Zamharir, M. Shahedi Asl, M. Ghassemi Kakroudi, N. Pourmohammadie Vafa, M. Jaberi Zamharir, Significance of hot pressing parameters and reinforcement size on sinterability and mechanical properties of ZrB2–25vol% SiC UHTCs, Ceram. Int. 41 (2015) 9628–9636. https://doi.org/10.1016/j.ceramint.2015.04.027.

[4] Q. Liu, W. Han, P. Hu, Microstructure and mechanical properties of ZrB2–SiC nanocomposite ceramic, Scr. Mater. 61 (2009) 690–692. https://doi.org/10.1016/j.scriptamat.2009.05.041.

[5] S. Guo, J. Yang, H. Tanaka, Y. Kagawa, Effect of thermal exposure on strength of ZrB2-based composites with nano-sized SiC particles, Compos. Sci. Technol. 68 (2008) 3033–3040. https://doi.org/10.1016/j.compscitech.2008.06.021.

[6] Y. Cao, H. Zhang, F. Li, L. Lu, S. Zhang, Preparation and characterization of ultrafine ZrB2–SiC composite powders by a combined sol–gel and microwave boro/carbothermal reduction method, Ceram. Int. 41 (2015) 7823–7829. https://doi.org/10.1016/j.ceramint.2015.02.117.

[7] X. Deng, S. Du, H. Zhang, F. Li, J. Wang, et al., Preparation and characterization of ZrB2–SiC composite powders from zircon via microwave-assisted boro/carbothermal reduction, Ceram. Int. 41 (2015) 14419–14426. https://doi.org/10.1016/j.ceramint.2015.07.077.

[8] S. Guo, Thermal and electrical properties of hot-pressed short pitch-based carbon fiber-reinforced ZrB2–SiC matrix composites, Ceram. Int. 39 (2013) 5733–5740. https://doi.org/10.1016/j.ceramint.2012.12.091.

[9] M. Shahedi Asl, M. Ghassemi Kakroudi, A processing-microstructure correlation in ZrB2–SiC composites hot-pressed under a load of 10 MPa, Univers. J. Mater. Sci. 3 (2015) 14–21. https://doi.org/10.13189/ujms.2015.030103.

[10] M. Khoeini, A. Nemati, M. Zakeri, M. Tamizifar, H. Samadi, Comprehensive study on the effect of SiC and carbon additives on the pressureless sintering and microstructural and mechanical characteristics of new ultra-high temperature ZrB2 ceramics, Ceram. Int. 41 (2015) 11456–11463. https://doi.org/10.1016/j.ceramint.2015.05.110.

[11] R.V. Krishnarao, Z. Alam, D.K. Das, V.V. Bhanu Prasad, G. Madhusudan Reddy, Pressureless sintering of (ZrB2–SiC–B4C) composites with (Y2O3+Al2O3) additions, Int. J. Refract. Met. Hard Mater. 52 (2015) 55–65. https://doi.org/10.1016/j.ijrmhm.2015.05.013.

[12] Z. Liu, C. Wei, P. Wang, S. Li, X. Ma, Z. Zhang, Enhanced mechanical properties of laminated ZrB2–SiC ceramics with porous Si3N4 interface, Ceram. Int. 46 (2020) 17003–17009. https://doi.org/10.1016/j.ceramint.2020.03.285.

[13] B.R. Golla, S.K. Thimmappa, Comparative study on microstructure and oxidation behaviour of ZrB2-20 vol% SiC ceramics reinforced with Si3N4/Ta additives, J. Alloys Compd. 797 (2019) 92–100. https://doi.org/10.1016/j.jallcom.2019.05.097.

[14] S.K. Thimmappa, B.R. Golla, V. Bhanu Prasad, B. Majumdar, B. Basu, Phase stability, hardness and oxidation behaviour of spark plasma sintered ZrB2-SiC-Si3N4 composites, Ceram. Int. 45 (2019) 9061–9073. https://doi.org/10.1016/j.ceramint.2019.01.243.

[15] Z. Ahmadi, B. Nayebi, M. Shahedi Asl, M. Ghassemi Kakroudi, I. Farahbakhsh, Sintering behavior of ZrB2–SiC composites doped with Si3N4: A fractographical approach, Ceram. Int. 43 (2017) 9699–9708. https://doi.org/10.1016/j.ceramint.2017.04.144.

[16] J. Zou, G.-J. Zhang, C.-F. Hu, T. Nishimura, Y. Sakka, et al., High-temperature bending strength, internal friction and stiffness of ZrB2–20vol% SiC ceramics, J. Eur. Ceram. Soc. 32 (2012) 2519–2527. https://doi.org/10.1016/j.jeurceramsoc.2012.01.035.

[17] N. Pourmohammadie Vafa, M. Ghassemi Kakroudi, M. Shahedi Asl, Advantages and disadvantages of graphite addition on the characteristics of hot-pressed ZrB2–SiC composites, Ceram. Int. 46 (2020) 8561–8566. https://doi.org/10.1016/j.ceramint.2019.12.086.

[18] M. Shahedi Asl, A. Sabahi Namini, S.A. Delbari, Q. Van Le, M. Shokouhimehr, M. Mohammadi, A TEM study on the microstructure of spark plasma sintered ZrB2-based composite with nano-sized SiC dopant, Prog. Nat. Sci. Mater. Int. 31 (2021) 47–54. https://doi.org/10.1016/j.pnsc.2020.11.010.

[19] Z. Ahmadi, B. Nayebi, M. Shahedi Asl, M. Ghassemi Kakroudi, Fractographical characterization of hot pressed and pressureless sintered AlN-doped ZrB2–SiC composites, Mater. Charact. 110 (2015) 77–85. https://doi.org/10.1016/j.matchar.2015.10.016.

[20] M. Shahedi Asl, M. Ghassemi Kakroudi, R. Abedi Kondolaji, H. Nasiri, Influence of graphite nano-flakes on densification and mechanical properties of hot-pressed ZrB2–SiC composite, Ceram. Int. 41 (2015) 5843–5851. https://doi.org/10.1016/j.ceramint.2015.01.014.

[21] M. Shahedi Asl, M. Ghassemi Kakroudi, Characterization of hot-pressed graphene reinforced ZrB2–SiC composite, Mater. Sci. Eng. A. 625 (2015) 385–392. https://doi.org/10.1016/j.msea.2014.12.028.

[22] M. Shahedi Asl, F. Golmohammadi, M. Ghassemi Kakroudi, M. Shokouhimehr, Synergetic effects of SiC and Csf in ZrB2-based ceramic composites. Part I: densification behavior, Ceram. Int. 42 (2016) 4498–4506. https://doi.org/10.1016/j.ceramint.2015.11.139.

[23] M. Shahedi Asl, B. Nayebi, Z. Ahmadi, P. Pirmohammadi, M. Ghassemi Kakroudi, Fractographical characterization of hot pressed and pressureless sintered SiAlON-doped ZrB2–SiC composites, Mater. Charact. 102 (2015) 137–145. https://doi.org/10.1016/j.matchar.2015.03.002.

[24] Z. Zhang, Y. Liu, Y. Yang, B.I. Yakobson, Growth Mechanism and Morphology of Hexagonal Boron Nitride, Nano Lett. 16 (2016) 1398–1403. https://doi.org/10.1021/acs.nanolett.5b04874.

[25] M.S. Bresnehan, M.J. Hollander, M. Wetherington, K. Wang, T. Miyagi, et al., Prospects of direct growth boron nitride films as substrates for graphene electronics, J. Mater. Res. 29 (2014) 459–471. https://doi.org/10.1557/jmr.2013.323.

[26] I. Farahbakhsh, Z. Ahmadi, M. Shahedi Asl, Densification, microstructure and mechanical properties of hot pressed ZrB2 –SiC ceramic doped with nano-sized carbon black, Ceram. Int. 43 (2017) 8411–8417. https://doi.org/10.1016/j.ceramint.2017.03.188.

[27] T. Ohtsuka, H. Mabuchi, H. Tsuda, K. Morii, Fabrication of Si3N4/SiC Composite Ceramics by Reactive Hot-Pressing from Elemental Powders, J. Japan Soc. Powder Powder Metall. 45 (1998) 321–325. https://doi.org/10.2497/jjspm.45.321.

[28] I.G. Talmy, J.A. Zaykoski, M.M. Opeka, High-Temperature Chemistry and Oxidation of ZrB2 Ceramics Containing SiC, Si3N4, Ta5Si3, and TaSi 2, J. Am. Ceram. Soc. 91 (2008) 2250–2257. https://doi.org/10.1111/j.1551-2916.2008.02420.x.

[29] M. Mallik, K.K. Ray, R. Mitra, Effect of Si3N4 Addition on Compressive Creep Behavior of Hot-Pressed ZrB2-SiC Composites, J. Am. Ceram. Soc. 97 (2014) 2957–2964. https://doi.org/10.1111/jace.13022.

[30] L. fa, Z. dongmei, S. xiaolei, Z. wancheng, Properties of hot-pressed of SiC/Si3N4 nanocomposites, Mater. Sci. Eng. A. 458 (2007) 7–10. https://doi.org/10.1016/j.msea.2007.01.126.

[31] M. Shahedi Asl, B. Nayebi, M. Shokouhimehr, TEM characterization of spark plasma sintered ZrB2–SiC–graphene nanocomposite, Ceram. Int. 44 (2018) 15269–15273. https://doi.org/10.1016/j.ceramint.2018.05.170.

[32] M. Shahedi Asl, A statistical approach towards processing optimization of ZrB2–SiC–graphite nanocomposites. Part I: Relative density, Ceram. Int. 44 (2018) 6935–6939. https://doi.org/10.1016/j.ceramint.2018.01.122.